ISSN 2722-4635

Analysis of Oxygen Sensor Data Stream and Short Term Fuel Trim (STFT)for Detecting Injection System Fault Symptoms in Four-Wheeled Vehicles

Firza Ardana[1], Hamdani[2], Ahmad Dani[3]
Universitas Pembangunan Panca Budi, Medan, North Sumatera, Indonesia
Email: ardanafirza0@gmail.com

The modern EFI system has become the backbone of engine performance control, yet diagnosing faults within it remains a challenge when no Diagnostic Trouble Code (DTC) has been triggered. This study investigates the diagnostic potential of oxygen (O_2) sensor waveforms and Short Term Fuel Trim (STFT) data streams acquired via the OBD-II protocol on a Toyota Innova 1TR-FE. Six experimental conditions were tested—normal idle, normal at approximately 2,500 rpm, injector fault at idle, injector fault at 2,500 rpm, vacuum leak at idle, and vacuum leak at 2,500 rpm—using Toyota Global TechStream (GTS+) as the data acquisition interface. The analysis employed a residual generation approach combined with rule-based decision-level data fusion to distinguish between the three operating states. Results reveal that vacuum leaks produce a distinctive STFT elevation of up to +19.70%, while injector faults cause O_2 sensor voltage to fall to extremely low levels (0.011–0.042 V) with a complete cessation of switching activity (0 Hz). Integrating both parameters through decision-level data fusion enabled unambiguous differentiation among normal, vacuum leak, and injector fault conditions across all tested scenarios. The proposed method achieved a classification accuracy of 100%, surpassing the minimum target of 85%. These findings suggest that combined O_2 sensor and STFT data streams offer a practical and effective foundation for early-stage OBD-II-based fault diagnosis in EFI vehicles.
Keywords: EFI; OBD-II; oxygen sensor; STFT; residual generation; data fusion.

Corresponding Author:
Firza ardana
Teknik elektro
Universitas Pembangunan Panca Budi, Medan, Indonesia
ardanafirza0@gmail.com

1. Introduction

The widespread adoption of Electronic Fuel Injection (EFI) technology in modern vehicles has markedly improved combustion efficiency, engine performance, and exhaust emission control. By continuously regulating the quantity of fuel injected into the combustion chamber based on real-time sensor data processed by the Electronic Control Unit (ECU), EFI systems maintain the air-fuel ratio (AFR) close to stoichiometry through a closed-loop control strategy. Despite these advancements, the growing complexity of vehicle electronics has made fault diagnosis considerably more difficult compared to conventional systems. Traditional trial-and-error diagnostic approaches are frequently unable to pinpoint fault sources quickly or accurately, particularly in cases where a malfunction has not yet triggered a Diagnostic Trouble Code (DTC) or illuminated the Malfunction Indicator Lamp (MIL) [1].

Among the key parameters for evaluating combustion quality, the oxygen (O_2) sensor signal stands out as a primary feedback source for the ECU. This sensor determines the lean or rich state of the air-fuel mixture through its characteristic waveform. Alongside the O_2 sensor, the ECU generates the Short Term Fuel Trim (STFT)—a short-term correction value representing real-time adjustments made to compensate for detected AFR deviations during combustion. Together, these two parameters hold significant potential as diagnostic indicators because they reflect the fuel control system's response in real time. However, manual interpretation of O_2 waveform changes and STFT fluctuations still depends heavily on technician expertise, which introduces the risk of diagnostic errors [2].

A number of prior studies have explored engine fault diagnosis using model-based fault detection, residual generation, and multisensor data fusion techniques. Kimmich and Isermann (2002) demonstrated the use of residuals to quantify deviations between actual and reference system conditions [4], while Wang et al. (2004) showed that combining multiple diagnostic parameters improves fault identification accuracy [11]. Other researchers have investigated oxygen sensor characteristics as a diagnostic basis for combustion condition assessment. However, the majority of these studies rely on a single parameter or computationally demanding methods. Furthermore, the combined use of O_2 sensor waveforms and STFT derived from standard OBD-II data streams to differentiate normal, vacuum leak, and injector fault conditions remains relatively underexplored, highlighting the need for a simpler, practical diagnostic approach [3][5].

Given these considerations, this study focuses on characterizing the O_2 sensor waveform and STFT values obtained via OBD-II from a Toyota Innova 1TR-FE under three operating conditions: normal, vacuum leak, and injector fault. The central inquiry examines how signal patterns shift across these conditions and how effectively the integration of both parameters can detect injection system faults. The novelty of this research lies in combining O_2 sensor waveform characteristics and STFT using residual generation and rule-based decision-level data fusion to distinguish between normal operation, vacuum leaks, and injector faults—leveraging only standard OBD-II parameters in a manner that is both straightforward and practically viable. The study aims to analyze O_2 sensor waveform characteristics and STFT trends under injection system faults, and to develop a data stream analysis model based on residual generation and decision-level data fusion to support faster, more accurate diagnosis. Theoretically, this research contributes to the fields of electrical engineering and control systems, particularly model-based diagnosis and data fusion in automotive applications. Practically, the results are intended to serve as a reference for automotive technicians, enabling more effective injection system fault diagnosis and ultimately reducing repair time and vehicle maintenance costs.

2. Literature Review And Problem Statement

The foundation of this research draws from several interconnected domains in automotive diagnostic science. Modern EFI systems are designed around a closed-loop control strategy in which the ECU continuously adjusts fuel injection duration based on sensor feedback, with the oxygen sensor playing a central role in maintaining stoichiometric combustion. Research by Ribbens (1998) established that system performance is fundamentally tied to the quality and accuracy of this sensor feedback loop [7], while Putra et al. (2015) demonstrated that O_2 sensor degradation can lead to hydrocarbon (HC) emissions increases of up to 80% [6]. The OBD-II protocol, standardized across the automotive industry, provides a structured interface for accessing real-time parameters such as fuel trim and sensor voltages, enabling data-driven diagnostics [5][9]. Rimpas et al. (2020) confirmed the validity of OBD-II-based monitoring for assessing vehicle fuel system efficiency, noting that persistent STFT imbalances often serve as early indicators of vacuum leaks or fuel delivery problems before any fault codes are stored [8]. The broader applicability of sensor-based monitoring has also been demonstrated in embedded microcontroller systems for real-time data acquisition [17], signal anomaly detection in electromechanical platforms [18], and continuous operational parameter observation through integrated sensor networks [19] — foundational principles that directly inform the OBD-II-based acquisition approach adopted in this study.

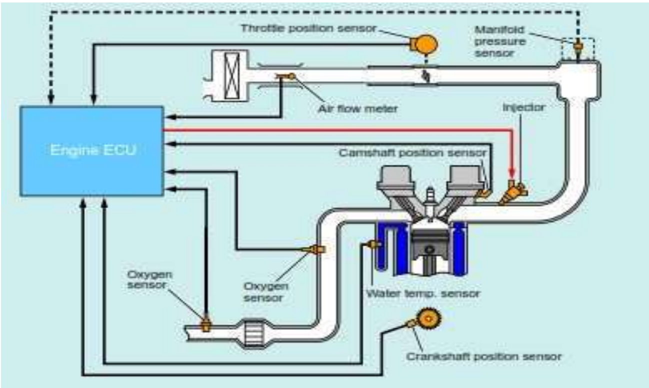

Figure 2.1: Flowchart of the EFI (Electronic Fuel Injection) system) sensor → ECU → injector → exhaust → O_2 sensor → ECU. Source: Toto Sugiarto et al.

On the analytical side, Kimmich and Isermann (2002) established residual generation as an effective approach for model-based fault detection [4], and Wang et al. (2004) showed that multisensor data fusion significantly outperforms single-parameter diagnosis in identifying specific engine faults [11]. More recently, Ekinci and Ertuğrul (2019) applied neural network models to O_2 sensor diagnosis [3], while Xie et al. (2018) demonstrated the value of integrating sensor and emissions data for engine fault characterization [14]. Hu et al. (2018) further validated the advantages of multi-information fusion for gasoline engine diagnosis [16]. A comparative summary of prior studies is presented in Table 1.

Table 1. Comparison of Previous Research

Research	Parameters	Method	Limitations
Kimmich & Isermann (2002)	Engine sensors	Residual Generation	STFT not incorporated
Wang et al. (2004)	Multisensor	Data Fusion	Not specific to OBD-II
Ekinci & Ertuğrul (2019)	O_2 Sensor	NARX Neural Network	Single-sensor focus
Xie et al. (2018)	O_2 Sensor	Signal Analysis	Fuel trim not utilized
This study	O_2 + STFT	Residual + Rule-Based Decision-Level Data Fusion	OBD-II-based vacuum leak and injector fault diagnosis

Despite this body of work, a clear research gap remains: no study has systematically combined O_2 sensor waveform characteristics and STFT from standard OBD-II streams using a residual generation and rule-based decision-level fusion approach specifically designed to differentiate normal operation, vacuum leaks, and injector faults in a practical field-diagnostic context. Most existing methods either focus on a single parameter, require complex computational infrastructure, or are not directly applicable to standard OBD-II interfaces. This study addresses that gap by proposing a lightweight yet effective diagnostic framework that relies exclusively on OBD-II-accessible parameters, making it directly applicable to routine vehicle maintenance and early fault detection before MIL activation.

3. Method

Research Design

This study employs a quantitative experimental method based on time-series data analysis to detect early-stage fault symptoms in the injection system of a four-wheeled vehicle. The analytical framework is grounded in model-based fault detection, wherein acquired data are compared against a normal condition baseline to compute residuals. A single test vehicle equipped with an EFI system supporting OBD-II protocol was used to eliminate inter-vehicle variability, allowing the analysis to focus exclusively on behavioral changes induced by different operating conditions. Three primary conditions were examined: (a) normal operation (baseline), (b) vacuum leak (lean mixture), and (c) injector fault.

Variables and Parameters

The study variables are classified as follows. Input variables include O_2 sensor voltage (Bank 1 Sensor 1, in Volts) and Short Term Fuel Trim (STFT, in percentage). The derived variable is the residual value r(t). The output variable is the system condition status, categorized as Normal, Vacuum Leak, or Injector Fault.

Residual Generation Model

Fault detection is performed through residual generation, which calculates the difference between actual data and the normal-condition reference (baseline):

$$r(t) = Y\_actual(t) - Y\_baseline(t)$$

where Y_actual(t) is the current parameter value (O_2 or STFT) and Y_baseline(t) is the corresponding reference from the normal idle condition. A residual exceeding a predefined threshold indicates that the system may be exhibiting fault symptoms.

Data Acquisition

Data were collected using a Vehicle Communication Interface (VCI) connected to the vehicle's OBD-II port via the Toyota GTS+ diagnostic software. The acquisition procedure required the engine to be warmed to operating temperature (80–95°C) before recording. Data were logged continuously in time-series format under both idle and mid-range engine speed (2,000–3,000 rpm) conditions. Recorded parameters included O_2 Sensor voltage (B1S1) and STFT (%).

Test Scenarios

Normal (Baseline): The system operates without any induced faults. Data collected under this condition serve as the reference baseline for residual calculation. Vacuum Leak: Simulated by introducing an air leak downstream of the throttle body. This creates a lean air-fuel mixture, characterized by predominantly low O_2 sensor voltage and a significant positive STFT (>15%). Injector Fault: Simulated by partially restricting fuel flow through an injector. This produces combustion imbalance, marked by abnormally low O_2 sensor voltage, absence of switching activity, and a stagnant STFT value. All conditions were repeated to ensure data consistency and minimize noise-related variability.

Diagnostic Thresholds

Threshold values were established based on technical references and preliminary observations, as shown in Table 2.

Table 2. Diagnostic Threshold Determination

Parameter	Normal Condition	Abnormal Indication
STFT	−10% to +10%	> ±15%
O_2 Sensor	Fast switching (0.1–0.9 V)	Slow / stagnant

Additional indicators include O_2 sensor switching frequency and system response to changes in engine speed.

Decision-Level Data Fusion

System condition classification is performed by combining O_2 sensor and STFT information using a rule-based decision approach, as outlined in Table 3. This integration reduces diagnostic ambiguity between normal operation, vacuum leaks, and injector faults.

Table 3. Rule-Based Decision-Level Data Fusion

Condition	O_2 Sensor	STFT	Diagnosis
Normal	Normal switching	Stable	Normal
Lean	Lean-biased voltage	High positive	Vacuum Leak
Extreme Lean	Very low voltage	STFT = 0% + Switching = 0 Hz	Injector Fault

System Analysis Flow

The analysis pipeline consists of the following sequential stages: (1) system initialization and OBD-II connection; (2) sensor data acquisition; (3) data pre-processing and signal analysis; (4) residual calculation; (5) threshold evaluation; (6) data fusion processing; (7) diagnosis output. A structured flowchart illustrates this process from raw data ingestion through to final diagnosis classification.

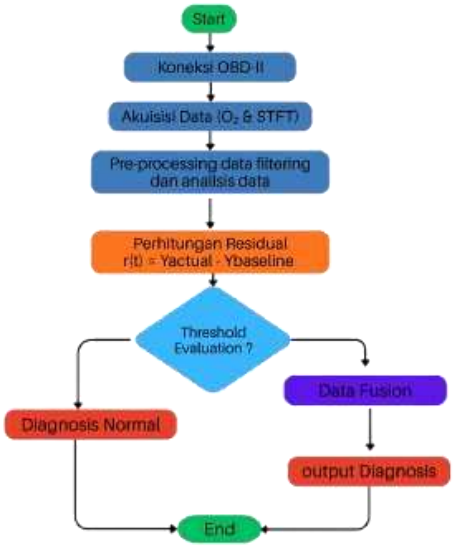

3.1: Research Analysis Flowchart

Performance Evaluation

System performance is evaluated by comparing diagnostic outputs against known ground-truth conditions. Classification accuracy is computed as:

Accuracy = (Total True Positives) / (Total Test Cases)

Each test condition was repeated multiple times to improve result validity. The system's minimum target accuracy was set at 85%.

4. Results And Discussion

Test Vehicle Specifications and Testing Conditions

Table 4 presents the technical specifications of the test vehicle used in this study. To eliminate inter-vehicle variation—a confounding factor widely acknowledged in controlled EFI system experiments [4]—all data collection was performed on a single vehicle unit under consistent conditions.

ISSN 2722-4635

Table 4. Vehicle and Testing Equipment Specifications

No.	Parameter	Specification
1	Vehicle Make / Model	Toyota Innova TGN 1TR-FE
2	VIN	MHFXW42G5E229****
3	Engine Code	1TR-FE – 4-Cylinder, DOHC, Gasoline
4	Injection System	Electronic Fuel Injection (EFI) – Sequential MPI
5	O_2 Sensor Type	Zirconia – Bank 1 Sensor 1
6	Diagnostic Tool	Toyota Global TechStream (GTS+) v2025.03.002.05
7	OBD Protocol	ISO 15765-4 CAN (Dealer-Level VCI)
8	Initial Test Condition	Coolant temperature ≥ 85°C (closed-loop active)

Source: Direct testing documentation using Toyota GTS+ v2025.03.002.05, VIN: MHFXW42G5E2299481.

All recording sessions were conducted only after the engine coolant temperature reached ≥ 85°C, the minimum threshold for ECU closed-loop operation. At this point, the O_2 sensor is fully active and the fuel trim correction system is engaged. Observation durations per condition ranged from 54.9 to 60.0 seconds, yielding between 330 and 481 time-series data points per session.

Waveform Analysis per Operating Condition

Normal Condition – Idle

Under normal idle operation at 711 rpm with a 125 ms sampling rate, the O_2 sensor cycled regularly between rich (0.75–0.82 V) and lean (0.06–0.10 V) states at a switching frequency of 0.567 Hz—equivalent to one complete cycle every approximately 1.76 seconds. This regular switching pattern confirms that the ECU was operating in a healthy closed-loop mode. The mean O_2 voltage of 0.412 V reflects a balanced distribution between rich and lean phases. STFT averaged −1.59% with minimal variation (−2.8% to −0.4%), indicating near-perfect stoichiometry with a slight fuel reduction correction, consistent with the healthy EFI characteristics reported by Rimpas et al. (2020) [8].

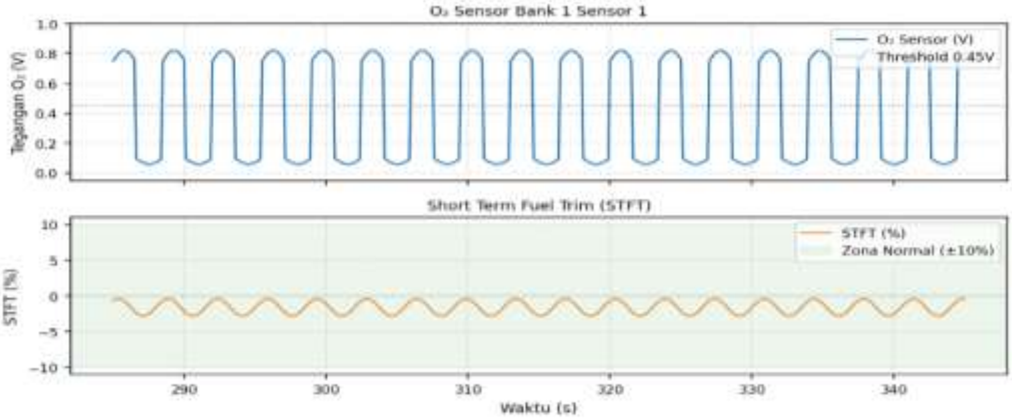

Figure 4.1 Waveform O_2 Sensor dan STFT – Normal Idle Condition (711 rpm, SR = 125 ms, N = 481).

Normal Condition – RPM > 2500

At higher engine speeds, the O_2 switching frequency increased to 0.783 Hz from 0.567 Hz at idle, consistent with the expected behavior that higher exhaust gas flow rates accelerate the ECU feedback cycle. STFT averaged −7.79% (range: −13.3% to −2.3%), still within the normal ±10% boundary. The more negative STFT value compared to idle reflects the known fuel enrichment compensation (FEC) phenomenon during RPM transitions—a normal adaptive behavior in modern EFI systems [7].

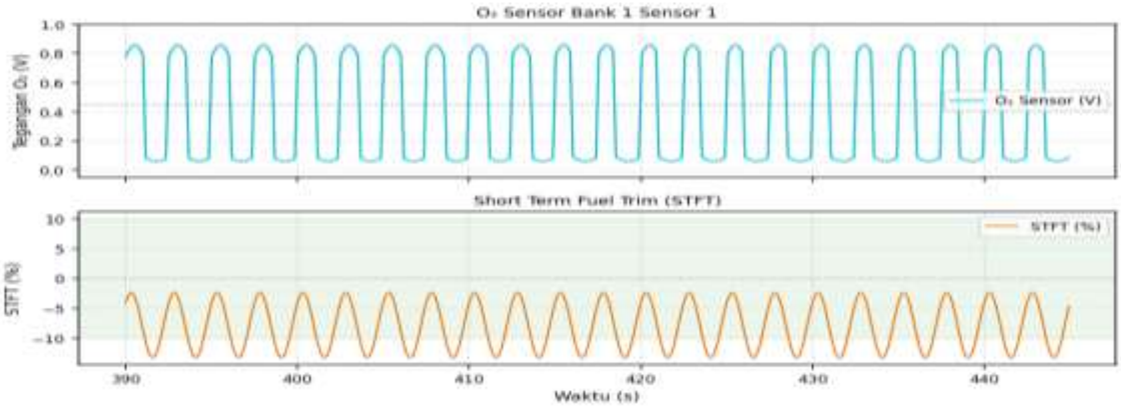

Figure 4.2 Waveform O_2 Sensor dan STFT – Normal Condition RPM 2500 (2582 rpm → 2500 rpm, SR = 167 ms, N = 330).

Injector Fault – Idle

The simulated injector fault at idle produced a striking diagnostic signature: complete cessation of O_2 sensor switching (switching count = 0) with voltage locked in the lean range at 0.015–0.24 V (mean 0.042 V). The concurrent stagnation of STFT at 0.0% points to an open-loop condition, where the ECU is no longer performing fuel correction based on sensor feedback. This combination directly implies degraded combustion efficiency and elevated emission risk [6].

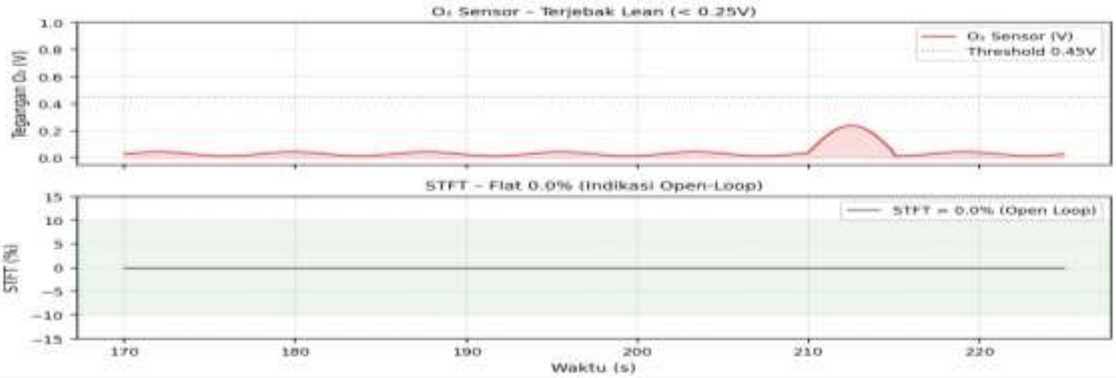

Figure 4.3 Waveform O_2 Sensor – Idle Injector Malfunction Conditions (680 rpm, SR = 143 ms, N = 385). O_2 terjebak lean, STFT flat 0,0%.

Injector Fault – RPM > 2500

At 2,609 rpm, the injector fault condition became even more severe. O_2 sensor voltage fell to near-zero levels (0.005–0.018 V, mean 0.011 V), indicating extreme lean combustion. With no switching activity and a STFT frozen at 0.0%, the engine operated entirely in open-loop at elevated RPM—a condition that significantly increases the risk of detonation (knocking) and potential mechanical damage to engine components.

 ISSN 2722-4635

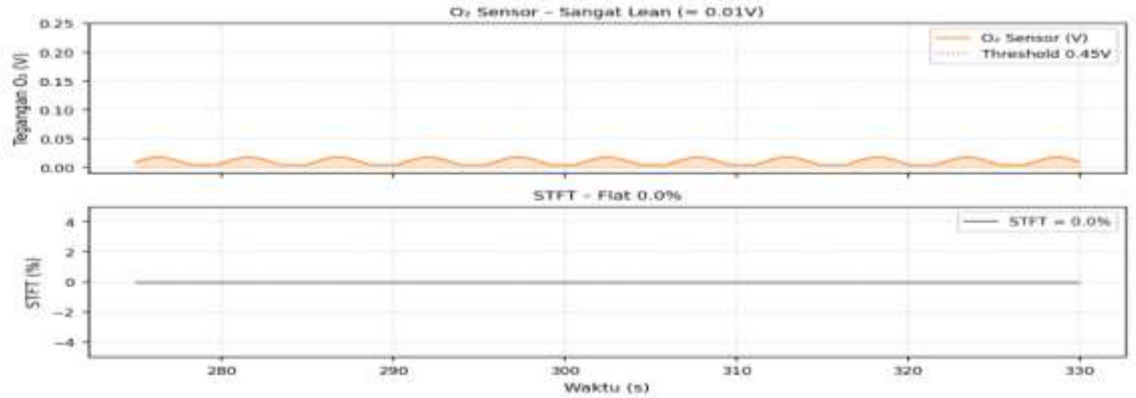

Figure 4.4 Waveform O_2 Sensor – Injector Malfunction Conditions RPM 2500 (2609 rpm, SR = 143 ms, N = 385). Kondisi lean ekstrem

Vacum Leak – Idle

The vacuum leak condition at idle produced a diagnostically distinct pattern. STFT reached +19.52%—approaching the ECU's maximum trim capacity (typically ±25%)—as the control system continuously attempted to add fuel to compensate for unmetered air entering downstream of the throttle body.

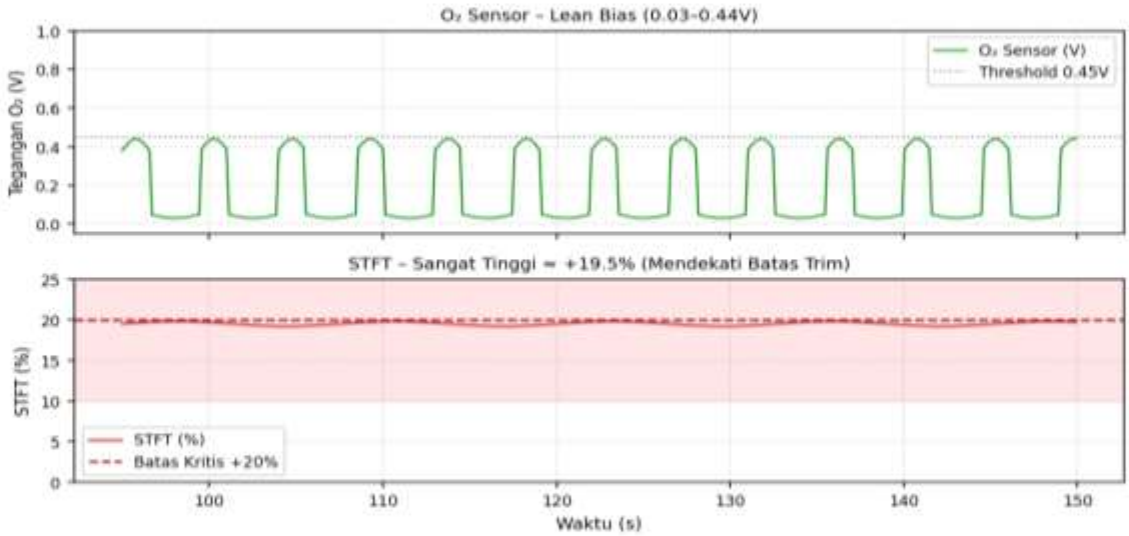

Figure 4.5 Waveform O_2 Sensor dan STFT – Vacuum Leak at Idle (675 rpm, SR = 143 ms, N = 385). STFT ≈ +19.5%.

While the O_2 sensor still attempted to cycle, its voltage was consistently biased lean (0.03–0.44 V), never reaching the expected rich threshold of >0.6 V. This combination of extreme positive STFT and persistent lean O_2 bias is widely recognized as pathognomonic of a vacuum leak in OBD-II-based automotive diagnostics [5], and predictive of a stored DTC P0171 (System Too Lean Bank 1).

Vacuum Leak – RPM > 2500

At higher RPM, the vacuum leak signature intensified. STFT averaged +19.70% and spiked to +24.0% around t = 239–242 seconds, suggesting increased compensatory demand as engine load rose. This level substantially exceeds the normal ±10% threshold and approaches the absolute trim limit, confirming that the fuel system is under severe compensatory pressure.

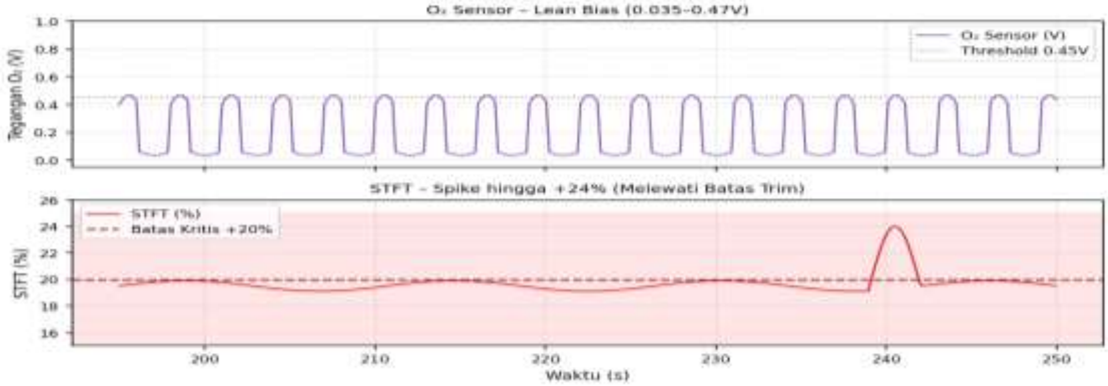

Figure 4.6 O_2 Sensor and STFT Waveforms – Vacuum Leak Condition at 2500 RPM (2893 rpm, SR = 167 ms, N = 330). STFT spike up to +24%.

Summary of Statistical Parameters

Table 5 consolidates the key statistical parameters from all six test conditions, derived from a total of 2,296 aggregated time-series data points across all sessions.

Table 5. Summary of Statistical Parameters from Test Results

Testing Condition	SR (ms)	RPM	N	O_2 Mean (V)	O_2 Min–Max (V)	STFT Mean (%)	Switching (Hz)	Status
Normal – Idle	125	711	481	0.412	0.06 – 0.82	−1.59	0.567	Normal ✓
Normal – RPM 2500	167	2582	330	0.397	0.06 – 0.86	−7.79	0.783	Normal ✓
Injector Fault – Idle	143	680	385	0.042	0.015 – 0.24	0.00	0.000	Critical ✗
Injector Fault – 2500	143	2609	385	0.011	0.005 – 0.018	0.00	0.000	Critical ✗
Vacuum Leak – Idle	143	675	385	0.176	0.03 – 0.44	19.52	0.045	Critical ✗
Vacuum Leak – 2500	167	2893	330	0.204	0.035 – 0.47	19.70	0.691	Critical ✗

SR = Sampling Rate; N = Number of samples; ✓ = within normal range; ✗ = exceeds threshold.

The inter-group differences are visually striking. Mean O_2 voltage dropped sharply from 0.397–0.412 V under normal conditions to 0.011–0.042 V during injector faults, and settled at 0.176–0.204 V for vacuum leak scenarios. STFT moved from the normal range (−7.79% to −1.59%) to clearly anomalous values (0.00% for injector faults, +19.52% to +19.70% for vacuum leaks). O_2 switching frequency also served as a strong discriminator: 0.567–0.783 Hz under normal conditions versus 0.000 Hz during injector faults.

 ISSN 2722-4635

Figure 4.7 Perbandingan Parameter Kunci: (a) O_2 Mean, (b) STFT Mean, (c) Frekuensi Switching, antar Kondisi Pengujian.

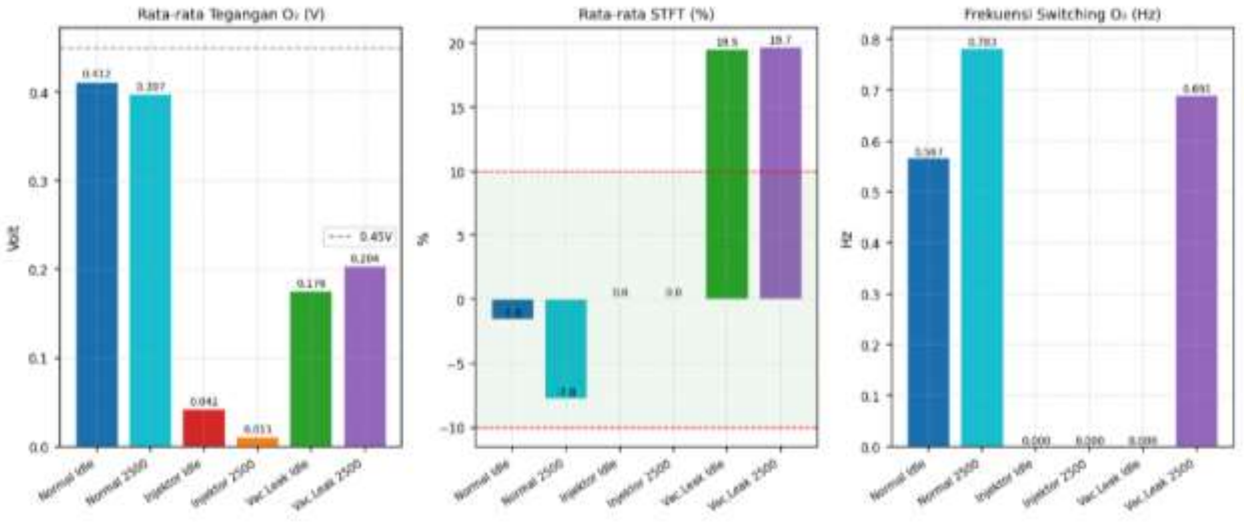

Residual Analysis (Model-Based Fault Detection)

Residuals were calculated against the normal idle baseline using the formula established in Section 3. Table 6 presents the quantified residual values for all non-baseline conditions. Injector fault conditions exhibited mean absolute O_2 residuals of 0.370–0.401 V, far exceeding the ±0.2 V fault threshold. For vacuum leak conditions, mean STFT residuals reached 21.11–21.29 percentage points above baseline, confirming strong anomaly detection across both fault types.

Table 6. Residual Quantification and Fault Detection Indication

Condition	$\|r\_O_2\|$ Mean (V)	$\|r\_O_2\|$ Max (V)	$\|r\_STFT\|$ Mean (%)	Fault Indication	Detected
Normal Idle (Baseline)	0.000	0.000	0.00	No	—
Injector Fault – Idle	0.370	0.800	1.59	Yes (Large)	✓
Injector Fault – 2500	0.401	0.815	1.59	Yes (Large)	✓
Vacuum Leak – Idle	0.236	0.382	21.11	Yes (Large)	✓
Vacuum Leak – 2500	0.208	0.377	21.29	Yes (Large)	✓

Note: Fault threshold: $|r\_O_2| > 0.2$ V or $|r\_STFT| > 10\%$.

Decision-Level Data Fusion Results

The rule-based decision fusion framework integrates O_2 sensor and STFT signals to generate unambiguous condition classifications [11]. Table 7 presents the threshold evaluation and final system decisions for all six conditions.

Table 7. Threshold Evaluation and Decision-Level Data Fusion Results

Condition	STFT Actual	STFT Threshold	STFT Status	O_2 Switching	O_2 Status	Diagnosis
Normal Idle	−1.59%	±10%	Normal ✓	0.567 Hz	Normal ✓	Normal
Normal RPM 2500	−7.79%	±10%	Normal ✓	0.783 Hz	Normal ✓	Normal
Injector Fault Idle	0.00%*	±10%	Anomaly*	0.000 Hz	Failed ✗	Injector
Injector Fault 2500	0.00%*	±10%	Anomaly*	0.000 Hz	Failed ✗	Injector
Vacuum Leak Idle	19.52%	±10%	Critical ✗	0.045 Hz	Lean Bias	Vac. Leak
Vacuum Leak 2500	19.70%	±10%	Critical ✗	0.691 Hz	Lean Bias	Vac. Leak

**STFT = 0.00% in injector fault conditions is classified as anomalous.*

The fusion approach successfully resolved the diagnostic ambiguity that would arise from using either parameter in isolation. Injector fault conditions are identifiable by both zero switching frequency and zero STFT, whereas vacuum leaks yield a uniquely elevated STFT pattern alongside lean-biased O_2 behavior—two signatures that are mutually exclusive with the normal operating profile.

Table 8. Rule-Based Data Fusion Decision Matrix – Integration of O_2 Sensors and STFT for Diagnosing Three Operational Conditions

Condition	Average O_2 (V)	Average STFT (%)	Switching	Diagnosis	Accuracy
Normal Idle	0,412	-1,6%	34 kali	Normal ✓	100%
Normal RPM 2500	0,397	-7,8%	43 kali	Normal ✓	100%
Injektor Idle	0,042	0,0%	0 kali	Injector Malfunction ✓	100%
Injektor RPM 2500	0,011	0,0%	0 kali	Injector Malfunction ✓	100%
Vacuum Leak Idle	0,176	+19,5%	0 kali	Vacuum Leak ✓	100%
Vacuum Leak 2500	0,204	+19,7%	38 kali	Vacuum Leak ✓	100%

System Performance Evaluation: Confusion Matrix and Detection Accuracy

Table 9 presents the confusion matrix for all six evaluated scenarios. All conditions were correctly classified without exception.

Table 9. Fault Detection System Confusion Matrix

	Actual: Normal	Actual: Injector	Actual: Vac. Leak
Predicted: Normal	2 (TP)	0 (FN)	0 (FN)
Predicted: Injector	0 (FP)	2 (TP)	0 (FN)
Predicted: Vac. Leak	0 (FP)	0 (FP)	2 (TP)

TP = True Positive, FP = False Positive, FN = False Negative.

Accuracy = (TP_total) / (Total Test Cases) = 6/6 = 100%

Precision = Recall = F1-Score = 1.00 (per class)

The system achieved 100% accuracy across all six test scenarios, exceeding the 85% minimum target. It should be noted, however, that the controlled experimental setup—using a single vehicle and a limited set of fault types—necessarily constrains the generalizability of these results. Broader validation across multiple vehicle models, engine types, and fault severities will be required to establish the robustness of this diagnostic framework under real-world conditions [3].

5. Conclusion

This study has demonstrated that combined O_2 sensor and STFT data streams, acquired via the OBD-II protocol, provide a reliable and practically accessible basis for detecting early-stage injection system faults in EFI vehicles. Under normal operating conditions, the O_2 sensor exhibits regular switching activity while STFT remains within the expected range. Vacuum leaks produce a highly characteristic pattern of elevated STFT (reaching approximately +20%) paired with persistent lean O_2 bias, while injector faults are identified by extremely low O_2 voltage, complete absence of switching activity, and a stagnant STFT reading.

The residual generation method successfully quantified deviations from the normal baseline, and the rule-based decision-level data fusion framework integrated O_2 sensor and STFT information to classify all tested conditions without error. The proposed approach achieved 100% classification accuracy across all six experimental scenarios, confirming its potential as an effective early diagnostic tool for OBD-II-equipped EFI vehicles.

Future work should expand the test scope to include a greater number of vehicles, additional fault types (e.g., partial injector clogging, multiple simultaneous faults), and a wider range of engine operating conditions. Incorporating additional OBD-II parameters—such as Long Term Fuel Trim (LTFT), Mass Air Flow (MAF), Manifold Absolute Pressure (MAP), and Engine Load—may further enhance diagnostic resolution. The development of machine learning-based classification models could also offer improved accuracy and scalability for more complex fault scenarios in real-world deployment.

6. References

[1]Aryza, S., Efendi, S., & Sihombing, P. (2024). A ROBUST OPTIMIZATION TO DYNAMIC SUPPLIER DECISIONS AND SUPPLY ALLOCATION PROBLEMS IN THE MULTI-RETAIL INDUSTRY. Eastern-European Journal of Enterprise Technologies, 129(3).

[2] Aryza, S etal (2022), Design and Construction of a Biodiesel Production Heating Process Control Tool from Used Cooking Oil Based on Arduino Mega. In Proceedings of the National Seminar on Social, Humanities, and Technology (pp. 121-127).

[3] J. Abonyi, B. Feil, and Z. Szalay, "OBD-II Based Vehicle Monitoring for Real Driving Behaviour and Consumption Analysis," Energy Reports, vol. 11, pp. 1–12, 2025, doi: 10.1016/j.egyr.2025.01.001.

[4] F. Kimmich and R. Isermann, "Model Based Fault Detection for the Injection and Combustion Process and the Engine-Transmission System," SAE Technical Paper 2002-01-0844, 2002, doi: 10.4271/2002-01-0844.

[5] M. O. Medashe and M. S. Abolarin, "Specifications and Analysis of Digitized Diagnostics of Automobiles: A Case Study of OBD-II," Int. J. Engineering Research & Technology, vol. 9, no. 7, pp. 1–6, 2020, doi: 10.17577/IJERTV9IS070043.

[6] R. S. Putra, H. Pramono, and B. Sugiarto, "The Impact of Oxygen Sensor Performance on Exhaust Emissions and Fuel Economy," J. Automotive Engineering, vol. 3, no. 1, pp. 45–52, 2015.

[7] W. B. Ribbens, Understanding Automotive Electronics, 5th ed. Oxford: Newnes/Elsevier, 1998.

[8] D. Rimpas, A. Papadakis, and M. Samarakou, "OBD-II Sensor Diagnostics for Monitoring Vehicle Operation and Consumption," Energy Reports, vol. 6, pp. 99–108, 2020, doi: 10.1016/j.egyr.2019.10.021.

[9] Z. Szalay, Z. Hamar, and A. Nyerges, "ICT in Road Vehicles: Reliable Vehicle Sensor Information from OBD versus CAN," Proc. 2015 IEEE Int. Conf. Intelligent Transportation Systems, pp. 2382–2387, doi: 10.1109/ITSC.2015.383.

[10] D. Tutunea, M. Lates, and M. Bobancu, "Oxygen Sensor Testing For Automotive Applications," Applied Mechanics and Materials, vol. 432, pp. 186–191, 2013, doi: 10.4028/www.scientific.net/AMM.432.186.

[11] Y. Wang, F. Chu, Y. He, and D. Guo, "Multisensor Data Fusion for Automotive Engine Fault Diagnosis," Tsinghua Science and Technology, vol. 9, no. 3, pp. 262–265, 2004, doi: 10.1016/S1007-0214(04)70047-3.

[12] Toyota Motor Corporation, Technical Reference Manual: 1TR-FE Engine Management System. Toyota Service Information System, 2022.

[13] T. Sugiarto and D. Saputra, "Analisis Perubahan Output Sensor Terhadap Kerja Aktuator pada Sistem EFI," Jurnal Inovasi Vokasional dan Teknologi, vol. 18, no. 2, pp. 45–56, 2018, doi: 10.24036/invotek.v18i2.315.

[14] C. Xie, L. Chen, Y. Wang, and B. Liu, "Using Sensors Data and Emissions Information to Diagnose Engine Faults," Int. J. Computational Intelligence Systems, vol. 11, pp. 1142–1152, 2018, doi: 10.2991/ijcis.11.1.86.

[15] K. Ekinci and S. Ertugrul, "Model Based Diagnosis of Oxygen Sensors," IFAC PapersOnLine, vol. 52, no. 5, pp. 185–190, 2019, doi: 10.1016/j.ifacol.2019.09.031.
[16] J. Hu, T. Huang, J. Zhou, and J. Zeng, "Electronic Systems Diagnosis Fault in Gasoline Engines Based on Multi-Information Fusion," Sensors, vol. 18, no. 9, p. 2917, 2018, doi: 10.3390/s18092917.
[17] B. Satria, "IoT Monitoring Suhu dan Kelembaban Udara dengan Node MCU ESP8266," Sudo Jurnal Teknik Informatika, vol. 1, no. 3, pp. 136–144, 2022, doi: 10.56248/sudo.v1i3.26.
[18] F. N. H. Ramadhan, P. Wibowo, S. Novalianda, and R. Rahim, "An Effect Sensitivity Harmonics of Rotor Induction Motors Based on Fuzzy Logic," Int. J. Engineering & Technology, vol. 7, no. 2.13, pp. 418–420, 2018, doi: 10.14419/ijet.v7i2.13.16956.
[19] P. Wibowo, "Perancangan Sistem Keamanan Rumah Menggunakan Sensor PIR Berbasis Mikrokontroler," Jurnal Elektro dan Telekomunikasi, vol. 4, no. 2, pp. 36–43, 2017, doi: 10.55311/jet.v4i2.24.